PHYSICAL REVIEW B

CONDENSED MATTER

THIRD SERIES, VOLUME 53, NUMBER 2 **1 JANUARY 1996-II**

RAPID COMMUNICATIONS

Rapid Communications are intended for the accelerated publication of important new results and are therefore given priority treatment both in the editorial office and in production. A Rapid Communication in **Physical Review B** *may be no longer than four printed pages and must be accompanied by an abstract. Page proofs are sent to authors.*

Dual alkali-metal-ion channel structures in poly(*p*-phenylenevinylene)

Guomin Mao and M. J. Winokur
Department of Physics, University of Wisconsin, Madison, Wisconsin 53706

F. E. Karasz
Department of Polymer Science and Engineering, University of Massachusetts, Amherst, Massachusetts 01003

(Received 18 September 1995)

X-ray-diffraction data from alkali-metal-doped poly(*p*-phenylenevinylene) (PPV) have been compared with various candidate structures ascertained by Harris [A. B. Harris, Phys. Rev. B **50**, 12 441 (1994)] in a mean-field study of a model Hamiltonian which includes polymer-polymer and guest-host (i.e., alkali-metal-ion to polymer chain) interactions. At least one of these recently identified phases is found to have a local ordering motif that is consistent with data from K- and Rb-doped PPV samples at the highest alkali-metal concentrations. A closely related structure is found to be consistent with data from Na-doped PPV. These two structures form a class of channel structures whereby the well-known single alkali-metal-ion array/threefold polymer chain structure is replaced by a lower symmetry structure characterized by a staggered pair of parallel quasi-one-dimensional alkali-metal-ion arrays surrounded by four polymer chains.

The structural ordering within conducting polymer guest-host compounds has received considerable attention[1–15] and this information continues to be centrally important for developing a deeper understanding of the properties displayed by this unique class of materials.[16] The pronounced compositional changes that accompany conducting polymer doping (or, more precisely, intercalation) are also mirrored by a rich array of structural phases and phase behavior. These structural phases have been often cast in the context of a staging mechanism[3,17] in analogy to the evolution within layered materials.[18,19] While some model systems show transformations conceptually consistent within the framework of staging,[5,6] there is indication that for many of the linear polymer hosts [e.g., polyacetylene (PA) and poly(*p*-phenylenevinylene) (PPV)], intercalated by smaller guest species (i.e., alkali-metal ions), much of the detailed behavior originates in the local degrees of freedom, especially rotational motions about the polymer chains axis.[20,21] This latter response is associated with the formation of various channel structures. This motif is marked by a quasi-one-dimensional construction wherein a single linear array of alkali-metal ions forms along the direction parallel to the polymer chain axis and these arrays are typically surrounded by either three[4,7] or four[3] polymer host chains. These basic structural units are often arranged to give trigonal,[8] tetragonal,[9] or orthorhombic[10] three-dimensional structures. A subset of these structural studies have convincingly shown the existence of systematic displacements by the polymer chains away from positions of high symmetry.[5,10–12] Detailed *ab initio* theoretical studies have also suggested structural distortions within the polymer chains themselves.[22]

Although the structural models based on this single-ion-column construction yield excellent fits to much of the experimental data, the less well-ordered structures[4,13,14] that form at the highest alkali-metal-ion concentrations within samples having threefold channel structures remain poorly understood. In this regime the alkali-metal concentrations can exceed twice those of the more ordered phases.[23] Equally significant are the changes in the scattering data. These data are far more difficult to assess and analyze because the pertinent scattering features broaden, shift position, and change their intensities with a complex functionality.[14]

Only a limited number of physical processes may account for this continued uptake of alkali-metal ions: (1) the alkali-metal-ion density per quasi-one-dimensional column increases; (2) the number of occupied channels increases; (3) there is a fundamental disruption of the channel structure to form new structural phases. This first scenario is inconsistent with existing experimental data. These data suggest only marginal changes in the intrachannel alkali-metal–ion-ion spacing. The second mechanism has been observed during electrochemical K doping of polyacetylene; a system dominated by fourfold channel structures. For systems displaying threefold channel structures there has been at least one unsuccessful attempt to incorporate this scheme.[14] Both these examples focus on the rotational response of the polymer chains within guest-host matrix as the dominating theme. The third cited process is difficult to describe in brief because it ostensibly invokes rotational and translational motions throughout the host matrix.

This paper presents a study of equatorial diffraction data from PPV films observed *in situ* during saturation doping by Na, K, and Rb alkali-metal vapors. We find this data can be successfully treated using a model which presumes an increase in the number of occupied channels through a systematic disruption of threefold channels to form adjacent nested pairs of one-dimensional alkali-ion arrays surrounded by four polymer host chains. Hence, this is evidence for the existence of striking structural reorganization by the alkali-metal-ion arrays *filling* these galleries. While there are considerable distortions within the guest-host matrix, this structural evolution still appears to be dominated by rotational motions of the polymer host about its chain axis. Moreover, these new phases bear a strong resemblance to a subset of structures generated during a mean-field study by Harris[21] using a representative Hamiltonian which embodies only rotational degrees of freedom.

Accounts of the sample preparation, experimental procedure, and modelling calculations have been reported previously.[10,24] In brief, uniaxially oriented samples of PPV multilayer thin films were sealed into x-ray capillaries with a small quantity of the appropriate alkali metal and then placed into an x-ray compatible two-zone furnace. The doping times often exceeded one week (or more) at these elevated temperatures ($\sim$230 °C for Rb and $\sim$290 °C for K and Na). X-ray-diffraction scans were performed using a Cu K_α (1.5421 Å) source and silicon-diode array detector. Conventional θ-2θ scans were acquired throughout the doping process.

The nominal packings, perpendicular to the polymer chain axis, for the host polymer and the threefold channel compounds are depicted in Figs. 1(a) and 1(b), respectively. In this two-dimensional (2D) representation the ellipsoidal planar rotors are identified with the projected polymer structure perpendicular to its chain axis. The uppercase letters in Fig. 1(a) identify the six possible channel sites that when filled, as shown by encircling one of these letter types in Fig. 1(b), yields a threefold channel in the $\sqrt{3}\times\sqrt{3}$ phase (or, equivalently, 120° phase). This form is observed in a myriad of guest/polymer-host systems,[4,7,8,13,15] and every filled alkali-metal-ion channel occupies lattice points of a 2D triangular Bravais lattice. The specific guest-host composition is dependent on the ion-ion intrachannel spacing versus that of the

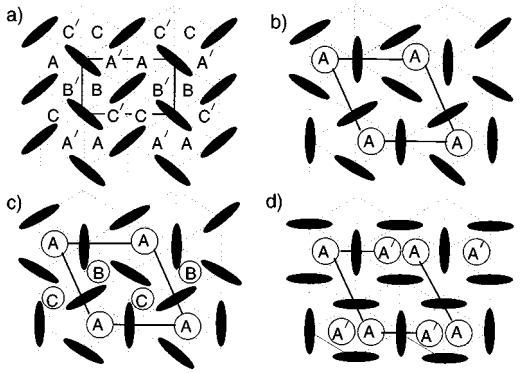

FIG. 1. Various template structures for the equatorial packing of the polymer chains and intercalant galleries assuming that the polymer chain axes approximate a triangular grid. (a) The herringbone (HB) phase of the pristine polymer superimposed with letters representing the sixfold degenerate 120° phase channel sites. (b) The intermediate alkali-metal/PPV $\sqrt{3}\times\sqrt{3}$ phase (or 120° phase). (c) Possible sites, **B** and **C**, for creation of additional threefold alkali-ion channels. (d) Alternative model showing disruption of threefold channels to form the 90° phase of Ref. 21 in which there is a pair of alkali-ion arrays surrounded by four polymer chains.

monomer unit repeat. For R_xPPV (R=Na, K, and Rb) the PPV c-axis repeat is approximately 6.6 Å and the ion-ion spacings are close to 4.4 Å. When combined with the three PPV chains/one ion channel packing motif, this results in a nominal $x=0.5$ value. Since these alkali-metal ions exhibit essentially complete ionization, the Coulomb repulsion between neighboring ions, within a channel, appears to be a significant component in preventing the wholesale factor of two reduction in the intrachannel ion-ion spacing necessary to double the guest-ion concentration using a single channel construction.

Figures 1(c) and 1(d) depict two possible pathways in which increasing alkali-metal content may be accommodated within the empirical paradigm that rotational degrees of freedom are centrally important. The first possibility is to forcibly fill unoccupied galleries at either the **B** or **C** positions through simple chain rotations and, thus, creating new threefold channels. This is conceptually equivalent to the ''stage 2'' to ''stage 1'' transition reported by Heiney *et al.*[5] for the fourfold channels of electrochemically dedoped K-PA. However there are two subtle differences in the threefold model; a secondary rotation by the entire original threefold channels about the alkali-metal-ion centers appears necessary for proper accommodation of the guest ions and the two possible sublattice sites, **B** and **C**, incur counterpropagating rotational responses. Modelling studies incorporating this type of structural evolution within a single-phase domain-wall picture have been relatively unsuccessful.[14] Our most recent attempts to model the experimental data using a two-phase coexistence of the 120° phase and structures based on the scheme shown in Fig. 1(c) have been equally unsuccessful[25] as well. At present it seems unlikely that this model has significant merit.

An alternate approach is to create side by side ion channels within each gallery using simple rotations by two of the three surrounding polymer chains as shown in Fig. 1(d). This yields a structure having two one-dimensional ion arrays

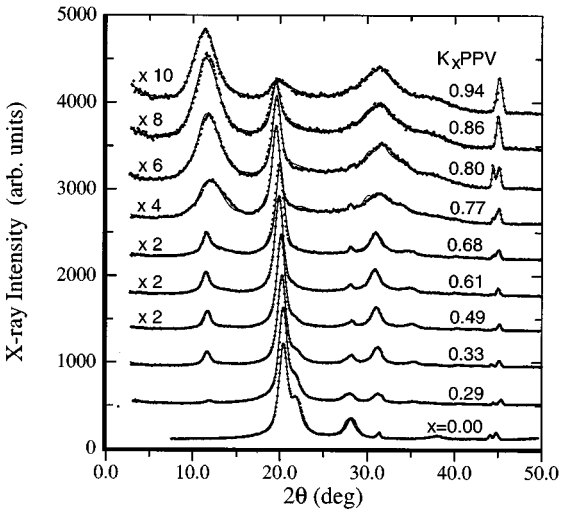

FIG. 2. Comparison of experimental (dots) and calculated (solid lines) equatorial ($hk0$) diffraction spectra throughout the entire K-vapor doping of PPV sequence. Each scan is labeled by its average K, x, composition (using the formula $K_xC_8H_6$). Sharp peaks near $2\theta = 32°$ and 45° are artifacts from crystalline salt impurities and the Be cell windows.

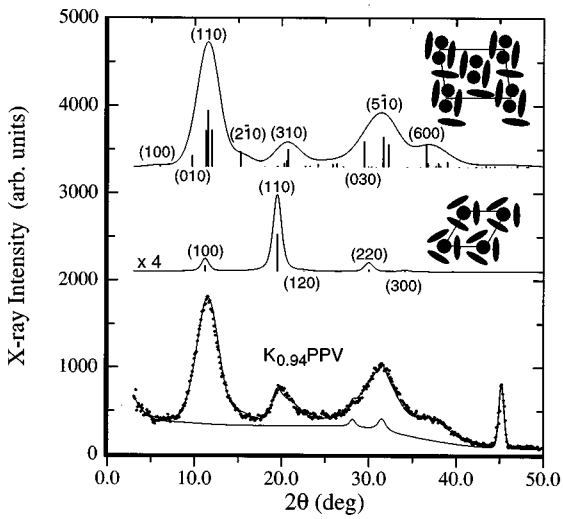

FIG. 3. Detailed view of the $K_{0.94}$PPV ($hk0$) spectrum showing (at bottom) the data (open circles) and calculated profile (solid line) as superimposed on a representative background. The middle profile (magnified $\times 4$) shows the 120° phase (middle inset) contribution and the top profile shows the ls-90° phase (top inset) contribution. Also shown are the most intense Bragg reflections (vertical bars) and their indices.

centered at the **A** and **A′** labelled positions. Symmetry equivalent structures are generated using the **B′** or **C′** sites. In this case the overall structure and symmetry of the channel becomes altered without necessarily changing the nominal triangular lattice repeat. This type of structural phase behavior has been explored in a number of mean-field theory investigations[20,21] and these studies have documented a rich number of interesting, thermodynamically stable structural phases. Of these, it is the 90° phase [Fig. 1(d)] which is relevant to our experimental data and forms the basis of the discussion that follows.

Figure 2 exhibits selected equatorial diffraction scans for the entire sequence during K-vapor doping. The first four scans, ''undoped'' to 0.49, can be effectively modelled using a two phase coexistence of the herringbone (HB) and 120° phases. The striking structural evolution seen at heavier K concentrations is captured in scans $x = 0.61$ through 0.94. The easily indexed 120° phase peaks, most pronounced in scan $x = 0.49$, are replaced by very broad, modest intensity scattering peaks centered near 2θ values of 11° and 32° and a weaker scattering feature at 21°. The final scan yields a scattering profile that is significantly different from that of the 120° phase. This can be most clearly discerned in the top two spectra shown in Fig. 3. Qualitatively analogous results are obtained during either Na or Rb vapor doping.

All of these latter profiles, $x > 0.49$, can be closely replicated by using a monotonically varying two-phase coexistence of the 120° phase and a modified 90° phase superimposed on a smooth background profile which represents a superposition of scattering from the glass cell, air, and any ''amorphous'' regions in the polymer films. Comparisons between the experimental data and calculated profiles are also contained in Fig. 2 and, in much greater detail, for selected ($hk0$) profiles from K-PPV, Rb-PPV, and Na-PPV in Figs. 3 and 4 (top and bottom) respectively. Table I lists the various 2D unit-cell parameters and relative compositions. To determine the relative phase fractions, ρ_i for ith phase, the following approximation is used,

$$\rho_i = \frac{I_i}{\Sigma_i I_i} \quad \text{and} \quad I_i = \int_{q_{\min}}^{q_{\max}} I_i(q) q^2 dq,$$

where I_i is the integrated scattering intensity from the ith phase and q is the associated scattering vector.

In all cases (including Na-PPV and Rb-PPV spectra not shown) all key scattering features are systematically reproduced, especially the pronounced loss of scattering intensity in the 2θ region spanning from 20° to 23° of the K-PPV and Rb-PPV spectra.

While the models of Fig. 1 and of Ref. 21 presume an undistorted triangular lattice, the attributes of each actual PPV guest-host system requires considerable structural modification of the ''90°'' phase. The explicit 2D representations are depicted in the insets of Figs. 3 and 4 for the three

TABLE I. Unit-cell parameters at selected compositions.

	HB		120°	ls-90°			ρ_i composition		
Alkali$_x$	**a**(Å)	**b**(Å)	**a**(Å)	**a**(Å)	**b**(Å)	γ(°)	ρ_{HB}	$\rho_{120°}$	$\rho_{ls-90°}$
$K_{0.00}$	8.11	5.15					1.00		
$K_{0.33}$	8.08	5.33	8.78				0.30	0.70	
$K_{0.49}$	8.10	5.43	8.81				0.12	0.88	
$K_{0.61}$			8.92	13.70	8.48	97.0		0.85	0.15
$K_{0.73}$			8.98	13.87	8.63	96.0		0.51	0.49
$K_{0.80}$			9.05	14.42	8.83	94.3		0.20	0.80
$K_{0.94}$			9.11	14.76	9.00	91.5		0.03	0.97
$Rb_{0.85}$			9.01	14.24	9.3	99.7		0.03	0.97
$Na_{0.89}$			8.66	13.86	8.90	86.3		0.12	0.88

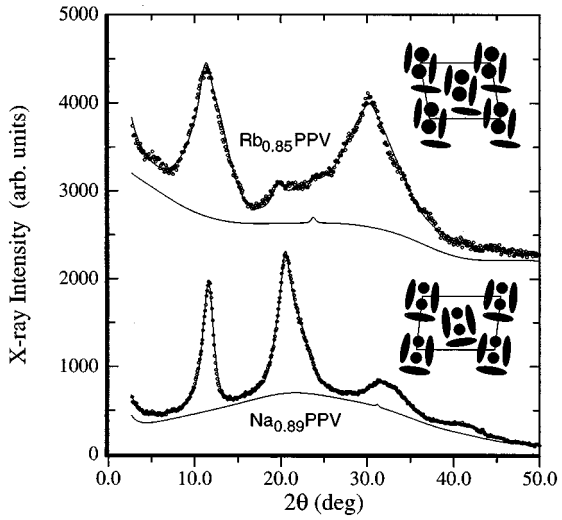

FIG. 4. Detailed views of $Rb_{0.85}PPV$ (at top) and $Na_{0.89}PPV$ (at bottom) ($hk0$) spectra showing the data (open circles), calculated profiles (solid lines) as superimposed on representative backgrounds using two different base models, ls-90° and ls-d-90° (top and bottom insets respectively).

differing alkali-metal ions studied. In all these cases the best-fit models require oblique 2D unit cells. To describe these lower symmetry (ls) structures we use the designation ls-90°. The distortion of the host lattice away from a triangular symmetry, implicit to the 120° phase, is not difficult to reconcile considering the overt lack of this symmetry in the base structural unit, two alkali-metal-ion channels surrounded by a rectangular cage of four polymer chains. In addition to the lower symmetry of the unit cells, these best fits also require rotational and translational displacements of the various unit cell components away from their nominal placement in the 90° phase. Since there are now twice as many filled channels, the effective planar (a-b plane) area per chain increases slightly when compared to that of the 120° phase. We also note that, to obtain these high-quality fits to the entire sequence of experimental data, small systematic variations, up to 5% or so, in the unit cell parameters are required. Some variation is expected simply because these *in situ* runs do not achieve true thermodynamic equilibrium. Hence the calculated alkali-metal compositions for each phase are found to slowly vary. Furthermore these PPV polymers themselves include significant intrinsic internal structural inhomogeneities. There are also marked reductions in the estimated crystallite coherence lengths during the transformation to the ls-90° phase. The estimated values for the 120° phase structures are 170, 150, and 120 Å for Na-, K-, and Rb-doped PPV respectively. These drop to 100, 50, and 35 Å in the respective ls-90° phases.

One final observation, which we highlight, is the intriguing difference in the local distortions of the "ls-90°" Na-PPV phase as compared to those of the K-PPV and Rb-PPV samples. This structure exhibits a subtle alternating left-right tilt of the polymer chains filling the unit cells reminiscent of the herringbone packing seen in pure PPV. Interestingly, an equivalent structure is also observed in the phase diagrams reported by Harris and it is designated the distorted d-90° phase (or, equivalently, ls-d-90° in the case of Na-PPV).

The presence of these doubly filled ion channels in combination with a strong ion-ion repulsion suggests that an intrachannel ordering between the paired array is needed. Preliminary scans which probe the nonequatorial scattering of the alkali-metal-ion structure yield data consistent with an out-of-phase staggered packing of the neighboring alkali-metal-ion arrays. Thus the nearest-neighbor spacing for ions within each channel drops from a nominal 4.4 Å (in the 120° phase) down to 3.8 Å in the dual channel structure.

In conclusion we have shown that variations on a simple theme, a transformation to a doubly filled channel, can explain the equatorial scattering spectra for all alkali-metal/PPV guest-host compounds exhibiting intermediate threefold channel structures. Furthermore, this evolution is shown to be conceptually consistent with the framework of the simplifying generalized anisotropic planar rotor models[21] which address only rotational degrees of freedom within the host-guest matrix. It remains to be seen whether or not these structural phases may be relevant for other conducting polymer guest-host compounds including those intercalated by the larger p-type (electron acceptor) dopants.

Financial support by NSF DMR Grant No. DMR-9305289 (G.M. and M.J.W.) is gratefully acknowledged. We would also like to thank Dong Chen for help in acquiring the the x-ray-diffraction spectra.

[1] R. H. Baughman, N. S. Murthy, and G. G. Miller, J. Chem. Phys. **79**, 515 (1983).

[2] N. S. Murthy, L. W. Shacklette, and R. H. Baughman, Phys. Rev. B **41**, 3708 (1990).

[3] R. H. Baughman *et al.*, Mol. Cryst. Liq. Cryst. **118**, 253 (1985).

[4] M. J. Winokur *et al.*, Phys. Rev. Lett. **58**, 2329 (1987).

[5] P. A. Heiney *et al.*, Phys. Rev. B **44**, 2507 (1991).

[6] D. Djurado *et al.*, Synth. Met. **34**, 683 (1990).

[7] D. Chen, M. J. Winokur, and F. E. Karasz, Synth. Met. **41**, 341 (1991).

[8] N. S. Murthy, L. W. Shacklette, and R. H. Baughman, Phys. Rev. B **40**, 12 550 (1989).

[9] N. S. Murthy, L. W. Shacklette, and R. H. Baughman, J. Chem. Phys. **87**, 2346 (1987).

[10] D. Chen *et al.*, Phys. Rev. B **45**, 2035 (1992).

[11] J. P. Aime *et al.*, J. Phys. (Paris) Lett. **46**, L379 (1985).

[12] F. Saldi, D. Billaud, and M. LeLaurain, Mater. Sci. Forum **91**, 363 (1992).

[13] D. Chen, M. J. Winokur, M. Masse, and F. E. Karasz, Phys. Rev. B **41**, 6759 (1990).

[14] M. J. Winokur, P. Davis, and D. Chen, in *Chemical Physics of Intercalation II*, Vol. 305 of *NATO Advanced Study Institute, Series B: Physics*, edited by P. Bernier, J. Fischer, S. Roth, and S. Solin (Plenum, New York, 1993), p. 283.

[15] N. S. Murthy *et al.*, Solid State Commun. **78**, 691 (1991).
[16] S. Y. Hong and M. Kertesz, Phys. Rev. Lett. **64**, 3031 (1990); H. A. Mizes and E. M. Conwell, Phys. Rev. B **43**, 9053 (1991); E. M. Conwell, H. A. Mizes, and S. Jeyadev, *ibid.* **41**, 5067 (1990); J. L. Bredas and A. J. Heeger, Macromolecules **23**, 1150 (1990).
[17] L. W. Shacklette and J. E. Toth, Phys. Rev. B **32**, 5892 (1985).
[18] *Intercalation in Layered Materials*, edited by M. S. Dresselhaus (Plenum Press, New York, 1986).
[19] E. Mele, in *Chemical Physics of Intercalation II* (Ref. 14), p. 93.
[20] H.-Y. Choi and E. J. Mele, Phys. Rev. B **40**, 3439 (1989).
[21] A. B. Harris, Phys. Rev. B **50**, 12 441 (1994).
[22] R. Baughman, N. Murthy, H. Eckhardt, and M. Kertesz, Phys. Rev. B **46**, 10 515 (1992).
[23] J. H. Simpson *et al.*, Polymer **34**, 4595 (1993).
[24] T. J. Prosa *et al.*, Macromolecules **25**, 4364 (1992).
[25] Guomin Mao and M. J. Winokur (unpublished).